technologies

Article

Cross-Tier Interference Mitigation for RIS-Assisted Heterogeneous Networks

Abdel Nasser Soumana Hamadou [1,*], Ciira wa Maina [2] and Moussa Moindze Soidridine [3]

[1] Department of Electrical Engineering, Pan African University Institute for Basic Sciences Technology and Innovation (PAUSTI), Nairobi P.O. Box 62000-00200, Kenya
[2] Centre for Data Science and Artificial Intelligence (DSAIL), Dedan Kimathi University of Technology (DeKUT), Nyeri P.O. Box 657-10100, Kenya
[3] Faculty of Science and Techniques, University of Comoros, Moroni, Comoros
* Correspondence: nasser.abdel@students.jkuat.ac.ke

Abstract: With the development of the next generation of mobile networks, new research challenges have emerged, and new technologies have been proposed to address them. On the other hand, reconfigurable intelligent surface (RIS) technology is being investigated for partially controlling wireless channels. RIS is a promising technology for improving signal quality by controlling the scattering of electromagnetic waves in a nearly passive manner. Heterogeneous networks (HetNets) are another promising technology that is designed to meet the capacity requirements of the network. RIS technology can be used to improve system performance in the context of HetNets. This study investigates the applications of reconfigurable intelligent surfaces (RISs) in heterogeneous downlink networks (HetNets). Due to the network densification, the small cell base station (SBS) interferes with the macrocell users (MUEs). In this paper, we utilise RIS to mitigate cross-tier interference in a HetNet via directional beamforming by adjusting the phase shift of the RIS. We consider RIS-assisted heterogeneous networks consisting of multiple SBS nodes and MUEs that utilise both direct paths and reflected paths. Therefore, the aim of this study is to maximise the sum rate of all MUEs by jointly optimising the transmit beamforming of the macrocell base station (MBS) and the phase shift of the RIS. An efficient RIS reflecting coefficient-based optimisation (RCO) is proposed based on a successive convex approximation approach. Simulation results are provided to show the effectiveness of the proposed scheme in terms of its sum rate in comparison with the scheme HetNet without RIS and the scheme HetNet with RIS but with random phase shifts.

Keywords: RIS; HetNet; spectral efficiency; cross-tier interference; optimisation; MIMO

Citation: Soumana Hamadou, A.N.; wa Maina, C.; Soidridine, M.M. Cross-Tier Interference Mitigation for RIS-Assisted Heterogeneous Networks. *Technologies* **2023**, *11*, 73. https://doi.org/10.3390/technologies11030073

Academic Editors: Sotirios K. Goudos and Shaohua Wan

Received: 1 May 2023
Revised: 27 May 2023
Accepted: 7 June 2023
Published: 9 June 2023

1. Introduction

Future wireless communications will enable massive connectivity for mobile and fixed devices, which will require high demand for mobile data traffic on cellular networks in terms of data throughput and network capacity [1]. In order to respond to the requirements of high-transmission rates and quality of service (QoS) for 5G systems, multitier networks improve the spectrum efficiency and capacity of the systems by adopting a heterogeneous design with small cells and a macrocell tier [2]. High-spectrum efficiency (SE) is necessary to enable smooth communication in heterogeneous networks since the bandwidth resources become constrained as the number of cells grows [3]. Additionally, a multitier network with densely deployed cells experiences very high intercell interference as well as cross-tier interference, which may prevent macrocell users (MUEs) within the vicinity of small base stations (SBSs) from having a good signal-to-interference-plus-noise ratio (SINR) as well as reduce the network's capacity overall [4]. Recently, business and academics have both shown a lot of interest in a developing hardware technology called reconfigurable intelligent surfaces (RISs), which aims to address the aforementioned challenge in heterogeneous networks (HetNets) [5–11].

Specifically, RIS is a two-dimensional artificial surface made up of an array of discrete elements that can be controlled individually or collectively [12]. It is a novel method of controlling the previously uncontrollable wireless propagation medium.

RIS technologies are widely labelled in the literature under names such as software-defined or hypersurfaces, intelligent walls, software-controlled metasurfaces, large intelligent surfaces or antennas, intelligent reflected surfaces (IRSs), and reconfigurable intelligent surfaces. The implementation of an RIS-assisted system is similar to the use case for half-duplex relays, with the key difference that RIS implements passive beamforming [13]. In this context, RIS-assisted communication can be used to improve the performance of traditional wireless communication systems by allowing more degrees of freedom via wireless channel control, resulting in a more relaxed set of constraints. Further, reconfigurable intelligent surfaces (RISs) can control the radio environment using low-noise amplification and do not require an analogue, digital, or power amplifier [13]. An RIS can modify the phase shift, the amplitude, or even the polarisation of the incident signal. Notably, the RIS technology is nearly passive in that it is entirely based on electromagnetic wave scattering and does require power amplifiers for signal transmission. Indeed, some energy is only required for the smart controller and for enabling the reconfigurability of the RIS. As a result, RIS can mitigate the interference or improve the signal quality at some specific and localised network locations. The RIS technology shows promising potential for applications in future networks, as it can partially control and shape the propagation channels as one desires. The deployment of RISs can be combined with existing technologies, such as multiple-input multiple-output (MIMO) systems, heterogeneous networks (HetNets) systems, millimetre-wave (mmWave) communications, terahertz (THz) communications, machine learning (ML), and artificial intelligence (AI), for enhancing the performance of existing and future wireless networks [12–14].

In addition, RIS technology can be used in a heterogeneous network to assist communications by generating supplementary propagation paths, enhancing the characteristics of the existing paths, and mitigating interference. Additionally, the components of RIS are almost passive in that they passively filter incoming signals before passively reradiating them in the desired direction without the use of additional power. These are some additional defining qualities of RISs: RISs are built of materials that are inexpensive and are essentially passive. Due to their physical resemblance to mirrors, they may also be simply put on building facades, factory ceilings, and interior walls. Because of its capability to reconfigure signals, the RIS has some of the most advantageous use cases for line-of-site (LOS) paths or at the cell edge [15,16]. RIS neither amplifies nor decodes the incoming signal, unlike conventional relaying methods, such as amplify-and-forward (AF) and decode-and-forward (DF) relaying [15,17]. As a result, RIS contributes to the construction of a smart radio environment that may be adequately designed for inexpensive and energy-efficient communication in heterogeneous networks by offering essential flexibility. However, in reality, adaptive phase shifting requires some active components.

2. Related Works

Several studies have been published that examine RIS as a substitute for amplifying and forward (AF) relays in order to achieve high-performance gains in the spectrum and energy efficiency of future wireless networks. Specifically, the authors of [17] demonstrated that RIS-aided transmission can outperform the DF relaying protocol in terms of energy efficiency (EE) for high-rate communications. However, the main advantage of RIS in the network is the algorithm structure for managing the phase changes of the passive elements. By creating the phase shift controller using an alternating algorithm design, the authors of [18] examined a RIS-assisted cognitive radio (CR) communication strategy for optimising the achievable secondary user (SU) rate of the system. Moreover, the authors of [6] analysed the RIS-assisted dual-function radar communications (DFRC) scheme for increasing the system's secrecy rate through the use of a multi-eavesdropper, multi-cast, and multiantenna optimisation approach. Moreover, the performance of a RIS-aided single-cell wireless sys-

tem with a multiantenna access point and multiple single-antenna users was examined by the authors in [10]. In particular, they focused on the asymptotic performance, or RIS, with an essentially unlimited number of elements and contrasted it with a benchmark enormous multi-input-multi-output (MIMO) system without RIS. Moreover, in [4], the authors developed an adaptative hybrid scheme technique that combined time domain techniques using reduced power Almost Blank Subframe (ABS) and power control techniques to mitigate the cross-tier interference between the femto base station and the macrocell user near the femtocell. Results obtained from the simulation demonstrated that the proposed technique could increase the spectral efficiency of femtocells. The technique proposed in this study only considers cross-tier interference between the femto base station and macrocell users. However, the energy efficiency of this technique was not considered as well. Additionally, in [19], the authors formulated a heuristic scheme called the Quality Efficient Femtocell Offloading Scheme (QEFOS), which classifies the users into three categories: macrocell users, which experience low cross-tier interference; macrocell users, which experience high cross-tier interference; and femtocell users. Nonetheless, the cross-tier interference in the case where the femto users experience high cross-tier interference and co-tier interference was not considered. Moreover, in [20], the authors proposed a method to mitigate downlink cross-tier interference between macrocells and small cells. The proposed method is based on an extended cross-tier interference mitigation scheme that coordinates not only cross-tier interference from macrocell to small cell users but also from small cell to macrocell users, which consists of mitigating cross-tier interference from small cell to macrocell users without changing the pilot allocation. Furthermore, the authors of [21] suggested a resource allocation scheme for RIS-assisted heterogeneous networks with non-orthogonal multiple access to improve spectrum efficiency and transmission rate. The proposed resource allocation scheme optimisation is based on the alternating iteration approach and successive convex approximations. Nevertheless, this study did not consider the performance of the proposed method with respect to the user's location. Moreover, in [22], the authors investigated the performance of RIS-assisted wireless communication systems under co-channel interference in order to determine the closed-form expressions for the outage probability and channel capacity. However, this study did not actually take into consideration the RIS phase shift optimisation as well as the trade-off between transmit power and co-channel interference. Moreover, in [23], the authors developed a novel scheme for efficient multiple access in RIS-aided multi-user, multi-antenna systems. A comprehensive comparison of different schemes and configurations was presented in order to determine which scheme is better for the 6G paradigm. However, this study did not consider co-channel interference or inter-user interference. Moreover, the study in [24] presented a survey of the design and applications of an RIS for beyond 5G wireless networks. A comprehensive, detailed survey of RIS technology limitations in current research, related research opportunities, and possible solutions was presented. Moreover, the study in [16] compared the RIS-assisted system with the distributed antenna-aided system. However, the non-line-of-site link between the transmitter and receiver was not considered. In continuation of the same objective, in [25], the authors investigate the intelligent reflecting surface (IRS) for sum-rate maximisation in cognitive radio-enabled wireless powered communications networks. They proposed an alternating (AO)-based solution with a successive convex approximation (SCA) technique to solve the unconvex optimisation problem. The result of conventional cognitive radio enabled wireless-powered communications networks. Nevertheless, this study only considered cognitive radio-enabled wireless-powered communications networks. Apart from cognitive radio (CR), MIMO, and DFRC communications, RIS has been used in D2D and IoT communication systems. For example, in [5], the authors analysed the performance of a RIS-assisted IoT network using two resource allocation problems, namely, spectral efficiency and energy efficiency maximisation. In [7], the authors investigated an RIS-based unmanned aerial vehicle (UAV)-assisted non-orthogonal multiple access (NOMA) downlink scheme for maximising the sum rate of the system by using a deep deterministic policy gradient (DDPG) algorithm. However, except for the works in [19–22], where the authors

proposed to mitigate cross-tier interference in HetNets without taking the impact of the users and RIS location in the network into consideration, a study of cross-tier interference mitigation in RIS-assisted HetNet is necessary, especially for maximising system sum rate and network performance with respect to user location and RIS location. Therefore, in contrast to the aforementioned studies, in this work, we examine an RIS-assisted HetNet where the reflected link from RIS to the macrocell users (MUEs), as well as the reflected interference link from SBS-RIS-MUEs, are employed to mitigate interference from small cells (SBS). By optimising the sum rate of the networks while keeping in mind the limitations of transmitting beamforming at the macrocell base station (MBS) and phase shift coefficients at the RIS, the main goal of this work is to develop interference-aware heterogeneous networks.

3. Contribution

The main contributions are outlined in the list below:

1. We examine the maximisation of spectrum efficiency (SE) in an RIS-assisted HetNet using a system model in which the macrocell base station (MBS) communicates with its users through a direct link and a reflected link.
2. We investigate how RIS helps to resolve cross-tier interference issues in HetNet.
3. Because the formulated optimisation problem is not convex, we solve it by maximising the sum rate of the combined desired channel by extending a semidefinite relaxation technique.
4. Finally, to confirm the viability of the suggested technique, numerical analysis is carried out through computer simulations under real-world channel conditions. To specifically measure and support the SE of the specified framework. The number of RIS elements, the MUE's locations, and the number of SBS were all analysed. Furthermore, we compare the proposed algorithm with HetNets without RIS and HetNets with RIS but with random phase shifts.

The rest of the paper is organised as follows: In Section 4, we describe the scheme model under study; then, in Section 5, we formulate the problem and present the proposed optimisation method; in Section 6, the numerical and simulation results are presented; and finally, the paper concludes.

4. System Model

As shown in Figure 1, we consider a RIS-assisted HetNet wireless network system that comprises K macro base station users (MUEs) and M macro base station (MBS) antennas, where J SBSs with S antennas are deployed under the overlaid MBS, and the MBS and users communicate via a RIS with N elements that reflect the incident signal into a direct channel and a reflected channel.

The SBSs installed within the MBS network cause MBS users to experience cross-tier interference. RIS is deployed in the network to enable interference mitigation. Let the channel coefficient vector from the MBS to the k-th macrocell user (MUE) be defined as $h_k = [h_{1k}, \ldots, h_{Mk}]^T \in \mathbb{C}^{1\times M}$, where the direct channel coefficient matrix from the M MBS antennas to the K MBS users is $H = [h_1|\ldots|h_K] \in \mathbb{C}^{M\times K}$ for $m = 1, \ldots M$, and $k = 1, \ldots K$. The channel coefficient vector between the MBS and a RIS, as well as between the RIS and the k-th macrocell user, is represented as $g_n = [g_{1n}, \ldots, g_{Mn}]^T \in \mathbb{C}^{M\times 1}$, where $G = [g_1|\ldots|g_N] \in \mathbb{C}^{M\times N}$ is the channel coefficient matrix from the M MBS antennas to the RIS, and $f_k = [f_{1k}, \ldots, f_{Nk}]^T \in \mathbb{C}^{1\times N}$, respectively, where $F = [f_1|\ldots|f_K] \in \mathbb{C}^{N\times K}$ is the channel coefficient matrix between the RIS and all of the macrocell users, for $n = 1, \ldots, N$. The channel coefficient vector from the SBSs to the k-th MUE is denoted as $h_j = [h_{1k}, \ldots, h_{Jk}]^T \in \mathbb{C}^{1\times J}$, where the matrix of the direct channel between the SBSs and MUE is $H^S = [h_1|\ldots|h_J] \in \mathbb{C}^{J\times K}$ for $j = 1, \ldots J$, and the reflected channel coefficient vector from the SBSs to the RIS is denoted as $g_j = [g_{1n}, \ldots, g_{Jn}] \in \mathbb{C}^{J\times 1}$, where $G_S = [g_1|\ldots|g_J] \in \mathbb{C}^{J\times N}$ is the channel coefficient matrix between the SBSs and the RIS. The reflected interference channel vector from the SBSs-RIS link to the MUE is denoted as

$f_n = [f_{1k}, \ldots, f_{Nk}]^T \in \mathbb{C}^{1\times N}$. The signal of the MBS is $x_m = \sqrt{P_m}x_k$, and the signal of the SBS is $x_s = \sum_{j=1}^{J} \sqrt{P_j}x_j$. Let us define the phase shift matrix as a diagonal matrix as well $\Theta = \text{diag}(\theta_1, \theta_2, \ldots, \theta_N)$, where $\theta_n \in [0, 2\pi]$ is the phase shift at the nth element, where $\theta_N = \beta_n e^{j\theta_n}$ comprises an amplitude coefficient $\beta_n \in [0, 1]$. Since we aim to obtain the maximum designed signal, we set the amplitude coefficient as $\beta_n = 1$. Hence, the received signal at the k-MUE can be written as:

$$y_k = \left(h_k{}^T + f_k^T \Theta g_n\right)\sqrt{P_m}x_k + \left(h_j{}^T + f_n^T \Theta g_j\right)\sum_{j=1}^{J}\sqrt{P_J}x_j + \varepsilon \quad (1)$$

where x_k and x_j are the MBS and SBS transmitted signals, respectively, and ε is the noise which follows $\mathcal{CN}(0, \sigma^2)$. The transmission signals of the MBS and SBS satisfy $E\left[|x_k|^2\right] = 1$ and $E\left[|x_j|^2\right] = 1$. Using (1), the signal noise ratio at the k-th MUE is expressed as:

$$SNR_k = \frac{P_m\left|h_k{}^T + f_k^T \Theta g_n\right|^2}{\sum_{j=1 j\neq n j\neq k}^{J} P_j\left|h_j{}^T + f_n^T \Theta g_j\right|^2 + \sigma^2} \quad (2)$$

where P_m and P_j are the MBS- and SBS-transmitted power, respectively. Based on (2) the achievable rate of the k-th MUE, which is formulated as:

$$R_k = \log_2(1 + SNR_k) \quad (3)$$

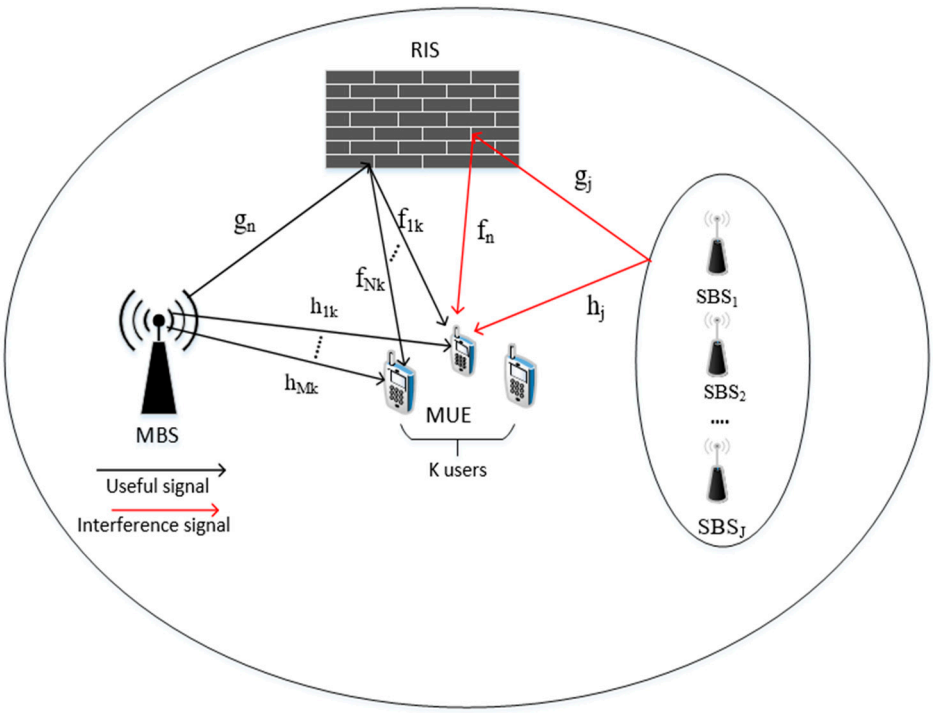

Figure 1. RIS-assisted HetNet system.

5. Problem Formulation

We aim to maximise the sum rate of the network by jointly optimising the transmit beamforming w and the phase shift matrix Θ, which can be represented as:

$$(\mathrm{P1}): \max_{W,\Theta} \sum_{k=1}^{K} R_k \tag{4}$$

$$\text{Subject to } \sum_{k=1}^{K} \|w_k\| \leq P, \tag{5}$$

$$0 \leq \theta_n \leq 2\pi, n = 1, \ldots N \tag{6}$$

The optimisation problem in (4) is non-convex because of the optimisation variables and the non-convex constraints in (6). We adapt Zero-Forcing-based transmit beamforming $W = \frac{\left(H^T+F^T\Theta G\right)^T}{\left(H^T+F^T\Theta G\right)\left(H^T+F^T\Theta G\right)^T}$, to the MBS to simplify the problem (4). In addition, the obtained transmit beamforming vector must be normalised by a factor of $\frac{\sqrt{P_m}\left(H^T+F^T\Theta G\right)^T}{\left\|H^T+F^T\Theta G\right\|}$ to fulfil the power constraint in (5). Accordingly, due to the non-concave objective function in (4), we propose to maximise the sum of the combined desired channel gain (CDC) of the MUE and the problem in (4) can be represented solely in terms of Θ, which is formulated as:

$$\max_{\Theta} \sum_{k=1}^{K} \left| {h_k}^T + f_k^T \Theta g_n \right|^2 \tag{7}$$

$$\text{Subject to } 0 \leq \theta_n \leq 2\pi, \forall_n \tag{8}$$

RIS Reflecting Coefficient-Based Optimisation (RCO)

Now, we optimise the reflecting coefficient Θ, and with the fixed transmit beamforming vector W, the optimisation problem (4) is reduced to (7). To ease the design, let us adopt a relaxation method to solve the problem (7) efficiently.

Defining $A = diag\left(f_k^T\right) \times g_n$, $\phi = \left[\phi_1, \quad \phi_2, \ldots, \quad \phi_n\right]^T$, where $\phi_n = e^{j\theta_n}$, (8) becomes:

$$|\phi_n| = 1, \forall_n \tag{9}$$

Problem (7) can be written as:

$$\max_{\phi} \sum_{k=1}^{K} \phi^T A A^T \phi + \phi^T A h_k + h_k^T A^T \phi + \left\| h_k^T \right\|^2 \tag{10}$$

$$\text{Subject to } |\phi_n|^2 = 1, \forall_n \tag{11}$$

Note that problem (10) is a non-convex quadratically constrained quadratic program (QCQP) problem, which can be converted into a homogeneous QCQP problem [26], by introducing an auxiliary variable t, hence problem (10) becomes:

$$\max_{\overline{\phi}} \sum_{k=1}^{K} \overline{\phi}^T B \overline{\phi} + \left\| h_k^T \right\|^2 \tag{12}$$

$$\text{Subject to } \left|\overline{\phi_n}\right| = 1, \ \forall_n \tag{13}$$

$$\text{Where } B = \begin{bmatrix} AA^T & Ah_k \\ h_k^T A^T & 0 \end{bmatrix}, \text{ and } \overline{\phi} = \begin{pmatrix} \phi \\ t \end{pmatrix} \tag{14}$$

But problem (12) is still non-convex, define $V = \overline{\phi}\overline{\phi}^T$, which must satisfy $rank(V) = 1$ and $V \succcurlyeq 0$, note that $\overline{\phi}^T B\overline{\phi} = trace(BV)$. We use semidefinite relaxation (SDR) to relax the non-convex nature of the rank-one constraint. Thus, problem (12) becomes:

$$\max_V \sum_{k=1}^{K} trace(BV) + \left\| h_k^T \right\|^2 \tag{15}$$

$$\text{Subject to } V_{n,n} = 1, \forall_n \tag{16}$$

$$V \succcurlyeq 0 \tag{17}$$

As problem (15) is a convex semidefinite program (SDP) problem, it can be solved by using the convex optimisation tool, such as CVX [27]. In general, the relaxed problem (15) may not yield a rank-one solution, implying that the optimal objective value of (15) only serves just an upper bound of (12). As a result, following [26], more steps are needed to construct the rank-one solution to problem (15). To be more specific, we first calculate the eigenvalue decomposition of V as $V = Z\Sigma Z^H$, where $Z = [e_1, \cdots, e_{N+1}]$ and $\Sigma = diag(\lambda_1, \cdots \lambda_2)$ are a unitary matrix and a diagonal matrix, respectively, both with size $(N \times 1) \times (N \times 1)$. Then, we calculate a suboptimal solution to (12) as $\overline{\phi} = Z\sqrt{\Sigma}r$, where $r \in \mathbb{C}^{(N+1)\times 1}$ is a random vector generated according to $r \in \mathcal{CN}(0, 1_{N+1})$ with $\mathcal{CN}(0, 1_{N+1})$ denoting the circularly symmetric complex Gaussian (CSCG) distribution with zero mean and covariance matrix 1_{N+1}, with independently generated Gaussian vectors r. The objective value of (12) is estimated as the maximum one reached by the best $\overline{\phi}$ among all r. Finally, the solution ϕ to problem (10) can be obtained by $\phi = e^{jarg\left(\left[\frac{\overline{\phi}}{\overline{\phi}_{N+1}}\right]_{(1:N)}\right)}$, where $[x]_{(1:N)}$ is the vector that contains the first N elements in x. According to [26], such an SDR technique followed by a sufficiently large number of randomizations guarantees an $\frac{\pi}{4}$ approximation of the objective value of (10).

6. Simulation Results

Simulation Setup

The MBS is deployed at the origin point (0, 0), the RIS is located at the coordinates (50, 0), the K MUE are placed randomly based on the uniform distribution in a (100, 100) rectangular space, and this uniform region is represented by a horizontal distance d, as illustrated in Figure 2, where U_k is the k-th MUE. We consider the case where the jth SBS is located at a distance of $(45(j+1), 0)$, where $j \in (1, 2, 3, 4)$. We assume that the direct path between an MBS and an MUE is dominated by non-line-of-sight (NLOS) components and so follows Rayleigh's fading. The channel is formed by $h \sim \mathcal{CN}(0, 1)$, where $\mathcal{CN}(\mu, \nu^2)$ is the circularly symmetric complex Gaussian (CSCG) distribution with mean μ and variance ν^2. RIS-related channels, on the other hand, employ Rician fading since we presume the RIS is positioned so that it is unobstructed by any obstructions and has line-of-sight (LOS) coverage with both MBS and MUE [5]. The simulation setup is shown in Figure 2.

The coverage radius of the macrocell and small cell is 500 m and 20 m [21], respectively. The distance-dependent path loss factor is given by [5]:

$$L(d) = C_0 \left(\frac{d}{D_0} \right)^{-\alpha} \tag{18}$$

where C_0 represents the pathloss at the reference distance, $D_0 = 1$ m and its value is influenced by the wavelength, the channel's quality, the antenna's gain, and the antenna's effective aperture. The distance between the MBS and MUE, the MBS and RIS, and the RIS

and MUE is represented by d, and the pathloss exponent is α. Specifically, the small-scale channel from the MBS to the RIS can be expressed as [10]:

$$G_m = \sqrt{L(d)}\left(\sqrt{\frac{\Omega}{\Omega+1}}\overline{H_m} + \sqrt{\frac{1}{\Omega+1}}\hat{H}_m\right) \tag{19}$$

where Ω is the Rician factor, and $\overline{H_m} \in \mathbb{C}^{M\times 1}$ and $\hat{H}_m \in \mathbb{C}^{M\times 1}$ are the LOS and NLOS components, respectively. While the LOS components are produced by $e^{-j\frac{2\pi}{\lambda}(d)}$ and the NLOS by a CSCG distribution. The channel between the RIS and the k-th MUE f_m is also subject to the same channel model, and it is modelled as [10]:

$$f_m = \sqrt{L(d)}\left(\sqrt{\frac{\Omega}{\Omega+1}}\overline{f_m} + \sqrt{\frac{1}{\Omega+1}}\hat{f}_m\right) \tag{20}$$

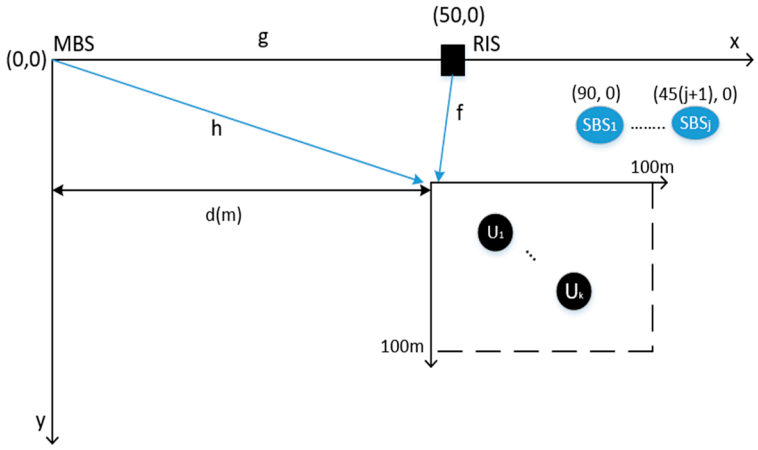

Figure 2. Simulation setup.

The distance between the MBS and RIS is 50 m. The distance between RIS and MUE is 5 m [21].

The detailed parameter setting is shown in Table 1.

Table 1. System parameters.

Parameters	Values
S	4
K	2
J	4
Center frequency	5 GHz [5]
σ^2	−60 dBm [7]
α	3 [21]
Ω	10 [7]
P_j	26 dBm [1]
P_m	40 dBm [1]
M	4
C_0	−30 dBm [5]

Now, in order to assess the effectiveness of the proposed HetNet networks scheme, we compare its SE performance to two reference scenarios:

- **Random phase shift**: In this example, we choose the phase shift at random in the range $[0, 2\pi]$, and then perform Zero-Forcing (ZF) at the MBS using the combined channel [5,7].

- **No RIS (Without RIS)**: In this plan, we mimic the network without RIS deployment. As a result, only the direct propagation path is included in the signal that the MUE has received.

In Figure 3, we evaluate the sum rate versus the number of elements of the RIS. It can be seen that the proposed scheme can achieve a higher performance gain compared to the other benchmarks. With an increasing number of RIS elements, the sum rate increases. This is not the case for the method without RIS, which is not impacted by the number of RIS elements. There are only minimal advantages when compared to the random phase shift approach. This demonstrates that using passive beamforming via RCO on a RIS-assisted HetNet network can mitigate cross-tier interference and increase the system sum rate.

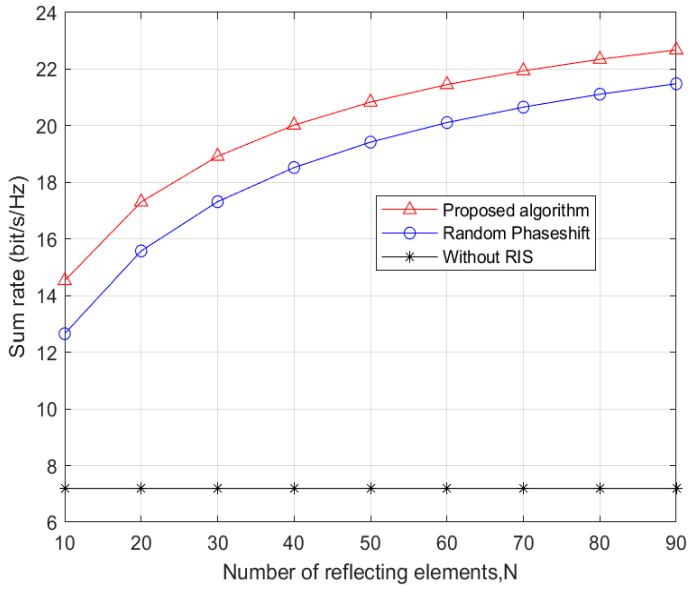

Figure 3. Sum rate vs. number of elements for d = 50 m.

Following that, in Figure 4, we compare the sum rate required by all schemes versus the distance between the MBS and the MUE. Specifically, we alter the distance between MBS and MUE while keeping the placement of the RIS constant and fixing N = 100.

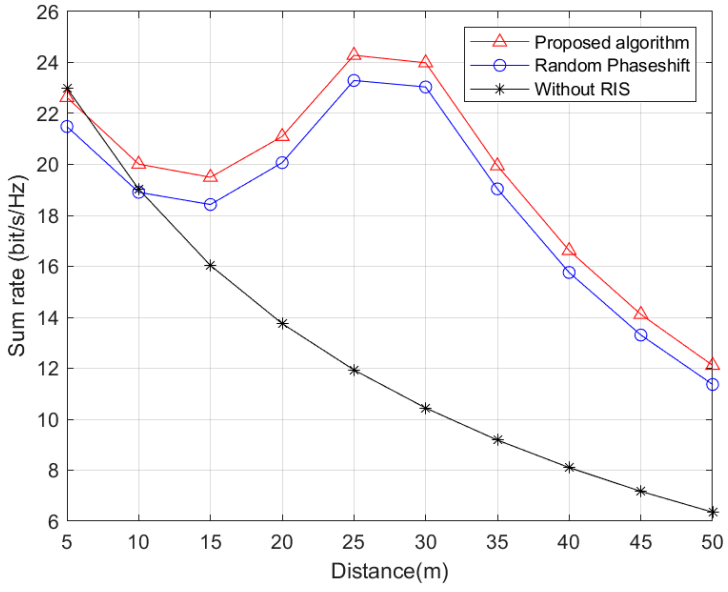

Figure 4. Distance vs. the sum rate N = 100.

In the scheme without RIS, it is first noted that the total rate drops as the distance increases. This is due to the pathloss that depends on distance. Second, we observed how the network performs with RIS support. As the distance grows, it is shown that the total rate first declines and then increases to achieve an ideal value before decreasing once more. Following is an explanation for this: When the MUE and MBS are close, the MBS's direct path takes precedence over the reflected path. However, when the distance increases, the reflected path begins to outperform the direct path. We can see at this point that the proposed technique outperforms the random situation. The RCO, in particular, gives a superior solution for phase shift at a distance of 25 m.

It is possible to deduce that deploying RIS can enhance the total rate of the RIS-assisted HetNet if the distance between RIS and MUE is between 24 and 34 m.

Figure 5 illustrates the total rate performance in proportion to MBS transmitted power. The graph indicates that, for any given transmit power, the proposed scheme produces a significantly higher total rate than the other two schemes. This indicates the efficiency of implementing RIS in a heterogeneous network (HetNet).

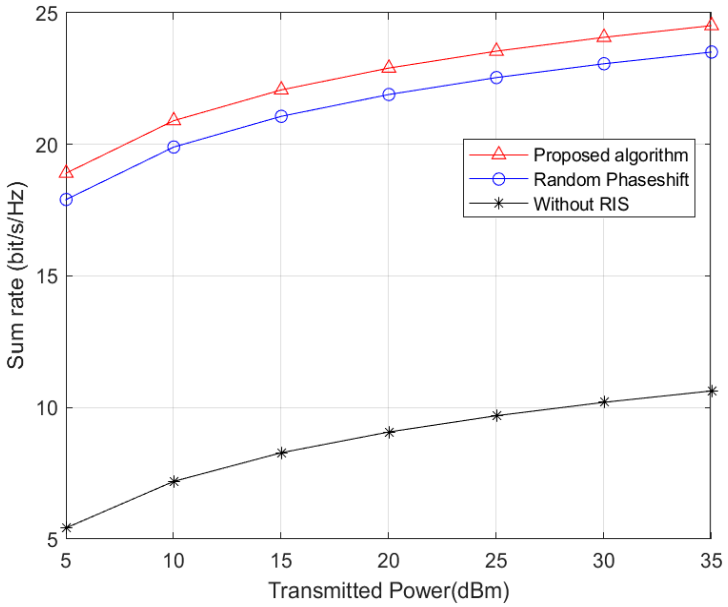

Figure 5. Transmit power versus sum rate N = 50, d = 50 m.

Finally, in Figure 6, we illustrate the overall rate as the number of small base stations (SBSs) increase when the distance between the MBS and the MUE is large and fixed at d = 200 m and the number of RIS elements is also large and fixed at N = 150. In terms of the total rate, the graph illustrates that the proposed scheme outperforms the baseline scheme. Furthermore, when the number of SBSs increase, the network's performance drops. This is because the number of SBS transmitters has increased. The drop also reflects the fact that passive beamforming at the RIS via a suitable phase shift design can mitigate interference caused by an increase in the number of small base stations (SBSs).

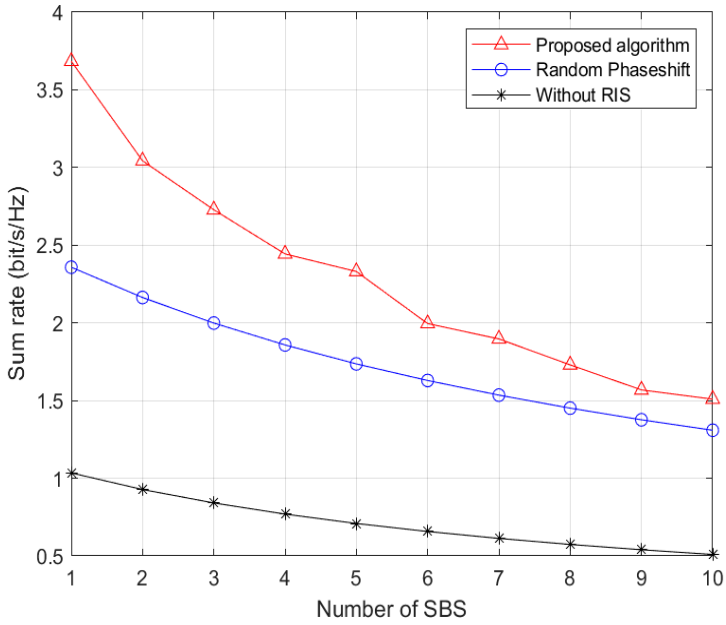

Figure 6. Number of SBSs vs. sum rate N = 150 and d = 200 m.

7. Conclusions

Surprisingly, there has been rising research and development activity on the reconfigurable intelligent surfaces (RISs) topic from both academia and industry working in antenna design, metamaterials, electromagnetics, signal processing, and wireless communications as a result of the increased potential of reconfigurable intelligent surfaces for wireless communications, as witnessed by the various recent proofs of concepts ranging from reflect arrays to intelligent antennas. Recently, the use of RIS in wireless communications networks has been promoted as a revolutionary method for transforming any wireless signal propagation environment into one that can be dynamically programmed for a variety of networking goals, including coverage extension, environmental perception, sensing, spatiotemporal focusing, and interference mitigation. In this paper, we have discussed an RIS-assisted HetNet to maximise the sum rate for macrocell users (MUEs). With respect to the total transmit beamforming constraint and realistic phase shift concerns, the MBS's transmit beamforming and the RIS's phase shifts were simultaneously optimised. To address the unconvex problem, we first adapted zero-forcing-based transmit beamforming to simplify the problem, and then we proposed to maximise the sum rate of the combined desired channel gain by efficiently applying reflection coefficient-based optimisation (RCO). The effectiveness of the proposed scheme was demonstrated by simulation results, which also provided some important insights into how to deploy RIS to obtain appropriate sum rate values in HetNet. Finally, the simulation results show that RIS can enhance the performance and reliability of HetNet systems.

Author Contributions: Conceptualization, A.N.S.H., C.w.M. and M.M.S.; methodology, A.N.S.H., C.w.M. and M.M.S.; software, A.N.S.H.; validation, A.N.S.H., C.w.M. and M.M.S.; formal analysis, A.N.S.H., C.w.M. and M.M.S.; investigation, A.N.S.H.; resources, A.N.S.H., C.w.M. and M.M.S.; data curation, A.N.S.H., C.w.M. and M.M.S.; writing-original draft preparation, A.N.S.H., C.w.M. and M.M.S.; visualization, A.N.S.H., C.w.M. and M.M.S.; supervision C.w.M. and M.M.S.; project administration, A.N.S.H.; funding acquisition, A.N.S.H. All authors have read and agreed to the published version of the manuscript.

Funding: This work is supported by the African Union (AU).

Institutional Review Board Statement: Not applicable.

Informed Consent Statement: Not applicable.

Data Availability Statement: The data used to support the findings of this study are available from the corresponding author upon request.

Conflicts of Interest: The authors declare no conflict of interest.

References

1. Nasser, A.; Muta, O.; Elsabrouty, M.; Gacanin, H. Interference Mitigation and Power Allocation Scheme for Downlink MIMO–NOMA HetNet. *IEEE Trans. Veh. Technol.* **2019**, *68*, 6805–6816. [CrossRef]
2. Nasser, A.; Muta, O.; Gacanin, H.; Elsabrouty, M. Non-Cooperative Game Based Power Allocation for Energy and Spectrum Efficient Downlink NOMA HetNets. *IEEE Access* **2021**, *9*, 136334–136345. [CrossRef]
3. Iqbal, M.U.; Ansari, E.A.; Akhtar, S. Interference Mitigation in HetNets to Improve the QoS Using Q-Learning. *IEEE Access* **2021**, *9*, 32405–32424. [CrossRef]
4. Kassim, A.Y.; Tekanyi, A.M.S.; Abdulkareem, H.A.; Muhammad, Z.Z.; Almustapha, M.D.; Abdu-Aguye, U.F. An Improved Cross-Tier Interference Mitigation Scheme In A Femto-Macro Heterogeneous Network. *J. Electr. Eng. Technol.* **2020**, *9*, 62–70.
5. Mondal, A.; Al Junaedi, A.M.; Singh, K.; Biswas, S. Spectrum and Energy-Efficiency Maximization in RIS-Aided IoT Networks. *IEEE Access* **2022**, *10*, 103538–103551. [CrossRef]
6. Mishra, K.V.; Chattopadhyay, A.; Acharjee, S.S.; Petropulu, A.P. OptM3Sec: Optimizing multicast IRS-aided multiantenna DFRC secrecy channel with multiple eavesdroppers. In Proceedings of the ICASSP 2022-2022 IEEE International Conference on Acoustics, Speech and Signal Processing (ICASSP), Singapore, 22–27 May 2022; pp. 9037–9041.
7. Jiao, S.; Xie, X.; Ding, Z. Deep Reinforcement Learning-Based Optimization for RIS-Based UAV-NOMA Downlink Networks (Invited Paper). *Front. Signal Process.* **2022**, *2*, 915567. [CrossRef]
8. Jian, M.; Alexandropoulos, G.C.; Basar, E.; Huang, C.; Liu, R.; Liu, Y.; Yuen, C. Reconfigurable intelligent surfaces for wireless communications: Overview of hardware designs, channel models, and estimation techniques. *Intell. Converg. Netw.* **2022**, *3*, 1–32. [CrossRef]
9. Mei, W.; Zheng, B.; You, C.; Zhang, R. Intelligent reflecting surface aided wireless networks: From single-reflection to multi-reflection design and optimization. *arXiv* **2021**, arXiv:2109.13641. [CrossRef]
10. Wu, Q.; Zhang, R. Intelligent Reflecting Surface Enhanced Wireless Network via Joint Active and Passive Beamforming. *IEEE Trans. Wirel. Commun.* **2019**, *18*, 5394–5409. [CrossRef]
11. Di Renzo, M.; Zappone, A.; Debbah, M.; Alouini, M.-S.; Yuen, C.; de Rosny, J.; Tretyakov, S. Smart Radio Environments Empowered by Reconfigurable Intelligent Surfaces: How It Works, State of Research, and The Road Ahead. *IEEE J. Sel. Areas Commun.* **2020**, *38*, 2450–2525. [CrossRef]
12. Fara, R.; Ratajczak, P.; Phan-Huy, D.T.; Ourir, A.; Di Renzo, M.; De Rosny, J. A prototype of reconfigurable intelligent surface with continuous control of the reflection phase. *IEEE Wirel. Commun.* **2022**, *29*, 70–77.
13. Pérez-Adán, D.; Fresnedo, Ó.; González-Coma, J.P.; Castedo, L. Intelligent Reflective Surfaces for Wireless Networks: An Overview of Applications, Approached Issues, and Open Problems. *Electronics* **2021**, *10*, 2345. [CrossRef]
14. Pei, X.; Yin, H.; Tan, L.; Cao, L.; Li, Z.; Wang, K.; Björnson, E. RIS-aided wireless communications: Prototyping, adaptive beamforming, and indoor/outdoor field trials. *IEEE Trans. Commun.* **2021**, *69*, 8627–8640.
15. Di Renzo, M.; Ntontin, K.; Song, J.; Danufane, F.H.; Qian, X.; Lazarakis, F.; De Rosny, J.; Phan-Huy, D.-T.; Simeone, O.; Zhang, R.; et al. Reconfigurable Intelligent Surfaces vs. Relaying: Differences, Similarities, and Performance Comparison. *IEEE Open J. Commun. Soc.* **2020**, *1*, 798–807. [CrossRef]
16. Kamaruddin, N.A.; Mahmud, A.; Bin Alias, M.Y.; Aziz, A.A.; Yaakob, S. Performance Evaluation of Reconfigurable Intelligent Surface against Distributed Antenna System at the Cell Edge. *Electronics* **2022**, *11*, 2376. [CrossRef]
17. Bjornson, E.; Ozdogan, O.; Larsson, E.G. Intelligent Reflecting Surface Versus Decode-and-Forward: How Large Surfaces are Needed to Beat Relaying? *IEEE Wirel. Commun. Lett.* **2019**, *9*, 244–248. [CrossRef]
18. Guan, X.; Wu, Q.; Zhang, R. Joint Power Control and Passive Beamforming in IRS-Assisted Spectrum Sharing. *IEEE Commun. Lett.* **2020**, *24*, 1553–1557. [CrossRef]
19. Agarwal, B.; Togou, M.A.; Ruffini, M.; Muntean, G.M. Mitigating the impact of cross-tier interference on quality in heterogeneous cellular networks. In Proceedings of the 2020 IEEE 45th Conference on Local Computer Networks (LCN), Sydney, Australia, 16–19 November 2020; pp. 497–502.
20. Kamiwatari, S.; Muta, O. Cross-tier interference mitigation considering pilot overhead for TDD MIMO heterogeneous networks. *IEICE Commun. Express* **2020**, *9*, 230–237. [CrossRef]
21. X, Y.; Yang, Z.; Huang, C.; Yuen, C.; Gui, G. Resource Allocation for Two-Tier RIS-Assisted Heterogeneous NOMA Networks. *ZTE Commun.* **2022**, *20*, 36–47.
22. Bian, Y.; Dong, D.; Jiang, J.; Song, K. Performance Analysis of Reconfigurable Intelligent Surface-Assisted Wireless Communication Systems Under Co-Channel Interference. *IEEE Open J. Commun. Soc.* **2023**, *4*, 596–605. [CrossRef]
23. Jiang, W.; Schotten, H.D. Orthogonal and Non-Orthogonal Multiple Access for Intelligent Reflection Surface in 6G Systems. In Proceedings of the 2023 IEEE Wireless Communications and Networking Conference (WCNC), Thessaloniki, Greece, 26–29 March 2023; pp. 1–6.

24. Okogbaa, F.C.; Ahmed, Q.Z.; Khan, F.A.; Bin Abbas, W.; Che, F.; Zaidi, S.A.R.; Alade, T. Design and Application of Intelligent Reflecting Surface (IRS) for Beyond 5G Wireless Networks: A Review. *Sensors* **2022**, *22*, 2436. [CrossRef] [PubMed]
25. Hameed, I.; Camana, M.R.; Tuan, P.V.; Koo, I. Intelligent Reflecting Surfaces for Sum-Rate Maximization in Cognitive Radio Enabled Wireless Powered Communication Network. *IEEE Access* **2023**, *11*, 16021–16031. [CrossRef]
26. So, A.M.-C.; Zhang, J.; Ye, Y. On approximating complex quadratic optimization problems via semidefinite programming relaxations. *Math. Program.* **2006**, *110*, 93–110. [CrossRef]
27. CVX: Matlab Software for Disciplined Convex Programming | CVX Research, Inc. Available online: http://cvxr.com/cvx/ (accessed on 20 April 2023).